ACS OMEGA

Open Access

http://pubs.acs.org/journal/acsodf

Article

Incorporating Transition Metal Ions into Uranium Oxide Hydrates: The Role of Zn(II) and the Effect of the Addition of Cs(I) Ions

Timothy A. Ablott,* Kimbal T. Lu, and Yingjie Zhang

Cite This: *ACS Omega* 2024, 9, 38284−38294

Read Online

ACCESS | Metrics & More | Article Recommendations | Supporting Information

ABSTRACT: The synthesis of two zinc-bearing uranium oxide hydrate (UOH) materials has been achieved, and their crystal structures, obtained via single-crystal X-ray diffraction using synchrotron radiation, and additional structural and spectroscopic properties are reported herein. Although both structures incorporate Zn^{2+} cations, the two differ significantly. The compound $Zn_2(OH)_2(H_2O)_5[(UO_2)_{10}UO_{14}(H_2O)_3]$ (**UOHF-Zn**), forming a framework-type structure in the $P\bar{1}$ space group, was composed of β-U_3O_8 layers pillared by uranyl polyhedra, with the Zn^{2+} cations incorporated within the framework channels. In contrast, the compound $Cs_2Zn(H_2O)_4[(UO_2)_4O_3(OH)_4]_2{\cdot}3H_2O$ (**UOH-Zn**) crystallized in the $Cmc2_1$ space group with a schoepite-like uranyl oxide hydroxide layered topology and both Zn^{2+} and Cs^+ cations making up the interlayer species. The apparent driving force for the differences in the structures was the change from KOH to CsOH during synthesis, with the smaller K^+ ions excluded in lieu of a higher proportion of Zn^{2+} (U/Zn ratio of 5.5:1) in **UOHF-Zn**, whereas in **UOH-Zn**, the larger Cs^+ ions were preferentially incorporated at the expense of fewer Zn^{2+} cations (U/Cs/Zn ratio of 8:2:1). Highlighted in this work is the effect of the chemical species and, in particular, their ionic radius on UOH formation, further improving the understanding of UO_2 alteration in the setting of deep geological repositories.

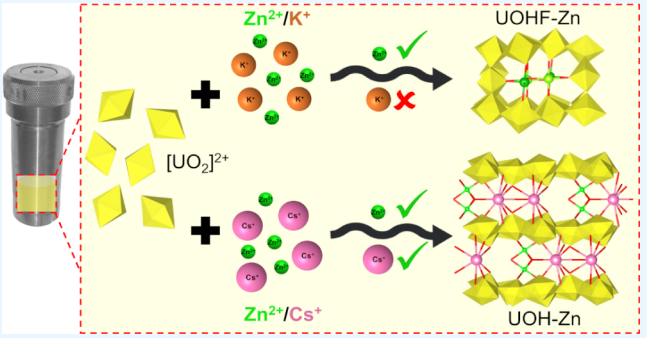

1. INTRODUCTION

The international drive toward combating climate change has seen nuclear energy gain renewed interest in recent years.[1] However, ever-present in the discussion around uranium oxide (UO_2) based nuclear fuel systems is the consideration of how to safely deal with the spent nuclear fuel (SNF) toward keeping both the general public and the environment safe in the centuries to follow.[2,3] As these considerations progress, many countries are looking to the storage of their SNF in deep, stable geological repositories.[4−6]

With UO_2 being the primary uranium species present in these repositories and the understanding that, if exposed to air or water, these materials can readily proceed along oxidation and hydration alteration pathways,[7,8] a major focus has been on further elucidating the chemistry of these systems. The most prevalent of these studies has been on the alteration of the mineral uraninite (UO_{2+x}), which is known to undergo oxidation from U^{4+} to U^{6+} under oxidative conditions.[9,10] The resultant uranyl species, $[UO_2^{2+}]$, are highly reactive and readily undergo interactions with their surroundings to form a plethora of uranyl oxide-based compounds.[11,12] These materials are typically composed of strongly bound axial oxygen atoms, as part of the uranyl bond of the UO_2^{2+} cation, and coordinated ligands that extend along the equatorial plane via bound O/OH groups. The result is typical uranium coordination geometries of tetragonal, pentagonal, and hexagonal bipyramids.[13,14] These uranium polyhedra extend through edge- and corner-sharing and often result in layered structures, wherein any additional metals taken up from their surroundings are incorporated as a secondary layer, which lies between these uranium sheets.[15,16]

One such subset of these materials are uranium oxide hydrate (UOH) compounds, which have been identified as forming during the early stages of the alteration of uraninite.[12] Given this, they have been proposed as a means of studying the alteration of UO_2-based SNF systems in geological repositories.[17] This focus has resulted in the identification of dozens of UOH-related mineral structures,[11,12,18] along with a growing library of synthetically produced UOH compounds.[15,19,20] The commonalities in these systems include recurring uranium oxide hydroxide sheet-like topologies, between which is found the interlayer cation species. The differentiating factors in these materials are 2-fold: the identity of the interlayer cations and the O/OH ratio of the uranium oxide hydroxide layer. In

Received: July 4, 2024
Revised: August 1, 2024
Accepted: August 16, 2024
Published: August 23, 2024

Table 1. Synthetic Uranium Oxide Hydrate Materials Containing Transition Metals

UOH−TM2^{2+}	chemical formula	space group	crystal structure?
UOF−KCd[32]	$Cd_1K_5(H_2O)_6[(UO_2)_{22}O_{23}(OH)_5]$	$C2/c$	yes
UOH−KCd[32]	$Cd_3K_2[(UO_2)_6O_9(OH)_2]$	$Pnnm$	yes
UOH−KNi[28]	$K_4Ni(OH)_3(H_2O)_9[(UO_2)_{12}O_7(OH)_{13}]$	$P3_1c$	yes
UOH−KCo[28]	$K_4Co(OH)_3(H_2O)_9[(UO_2)_{12}O_7(OH)_{13}]$	$P3_1c$	yes
UOH−Ni[40]	$[Ni(H_2O)_4]_3[U(OH,H_2O)(UO_2)_8O_{12}(OH)_3]$	$P\bar{1}$	yes
UOH−M (M = Mn, Zn, Ni, Co)[41]	$[Mn(H_2O)_4][(UO_2)_3O_3(OH)_2]\cdot H_2O$	$P\bar{1}$	yes

examining the identified interlayer cations, some trends are apparent. In naturally occurring UOH systems, the incorporated cations have been found to be mostly alkali[21,22] and alkaline earth[23,24] species, along with a prevalence of Pb-based minerals, expected given its position at the end of the U decay pathway.[25,26] Notably lacking are UOH minerals containing transition metals, despite their relative abundance in the Earth's crust. A means of filling the gaps in these UOH systems has thus been the generation of a range of synthetic UOH compounds, with alkali metals,[21] alkaline earth metals,[27] transition metals,[28] heavy metals,[29] and lanthanides[30] all identified as the secondary cation incorporated into these structures. Thus, this has proven to be an effective method to broaden the scope of possible UOH compounds as the alteration pathway of UO_2-based materials.

Upon examining these systems, what was also identified was a more complex substructure of the typical layered UOH structure, wherein the axial oxygens are also coordinated, acting as bridging ligands between the uranyl polyhedra layers to form framework-type structures, since termed uranium oxide hydrate frameworks (UOHFs). These frameworks give rise to channels that extend throughout the structure, and it is into these channels that the secondary cations are incorporated, with compounds containing Cs^+, Sr^{2+}, Cd^{2+}, Pb^{2+}, Y^{3+}, Er^{3+}, Sm^{3+}, Eu^{3+}, Gd^{3+}, and U^{4+} all identified.[27,29,31−35] This increased structural complexity further exemplifies the need to better understand the chemistry that impacts the formation of these UOH/F systems.

While minerals containing uranium and 3d transition metals have been identified, despite their abundance in the Earth's crust, there is a dearth of UOH minerals containing such species. This has been reasoned as possibly due to uranium-based minerals not being exposed to alteration conditions in the presence of such elements when proceeding along their paragenetic sequence.[15,36] However, in geological repositories, exposure to such elements and conditions would be much more likely to take place. In addition, transition metals will also be present in both the confinement vessels used for SNF storage and likely in the confinement matrix itself. Therefore, an understanding of the interaction of UOH phases with transition metals is critical.

There have been a small number of reported synthetic UOH compounds containing 3d transition metals (Table 1); however, with only a select few detailed crystal structures available, understanding the role of the transition metal cations in supporting the UOH structure has not been well established. One such 3d transition metal that warrants further study is zinc, with only the one reported study by Chernorukov et al. This sole example of a Zn-containing UOH material stands out given the 290 reported minerals containing Zn, 6 of which have been reported to contain both zinc and uranium.[37] Interestingly, in each of these 6 minerals, the U/Zn ratio is 1:1 or lower, with no reported structures containing uranium as the majority cation species. Given this would be the case in UOH-based compounds, the ability to study such materials is critical to provide unique insights into the uranium−zinc interactions which may occur in a geological repository setting.

An additional consideration is the added presence of K^+ ions as reported by Zhang et al. in the synthesis of UOH−KNi and UOH−KCo,[28] along with other UOH compounds containing 2+ metal ions reported to also incorporate Na^+ or K^+.[32,38] From this comes the need to better comprehend the role that monovalent cations play when introduced into these structures alongside 3d transition metals. Broadening this concept beyond Na^+ and K^+, cesium (Cs^+), given its presence in SNF systems as the long-lived ^{135}Cs isotope and evidence that it can be incorporated into uranium alteration products, also warrants additional study in this area.[31,39]

In this study, we report the syntheses of two novel UOH/F materials containing Zn^{2+} ions and explore the intricacies of their structures using structural and spectroscopic techniques. **UOHF-Zn** was isolated as a framework-type structure, with Zn^{2+} ions lying within the channels of the uranium backbone in a novel arrangement. In comparison, **UOH-Zn** was found to form a layered UOH-type material with both Zn^{2+} and Cs^+ cations present as the interlayer cation species, with the Cs^+ and Zn^{2+} ions acting as pillars, resulting in a pseudoframework type structure. With similar reaction conditions employed in both syntheses, changing the base from KOH for **UOHF-Zn** to CsOH for **UOH-Zn** gave rise to markedly different structures, highlighting the impact that additional monovalent cations present during formation can have on the resultant structure. In addition to exploring these structural features in detail, the microstructures and spectroscopic properties of both compounds were explored by using scanning electron microscopy and powder X-ray diffraction along with Raman and diffuse reflectance spectroscopies.

2. EXPERIMENTAL SECTION

2.1. Synthesis of Materials. Uranyl nitrate hexahydrate with natural isotopic ratios of uranium was used in the synthesis of the materials. Compounds with uranium are radioactive and should be handled in a regulated laboratory. All other chemicals of A.R. grade were from Sigma-Aldrich (Merck).

2.1.1. $Zn_2(OH)_2(H_2O)_5[(UO_2)_{10}UO_{14}(H_2O)_3]$ (UOHF-Zn). Zinc nitrate hexahydrate, $Zn(NO_3)_2\cdot 6H_2O$ (0.0982 g, 0.33 mmol), and uranyl nitrate hexahydrate (0.165 g, 0.33 mmol) were dissolved in 5 mL of deionized (DI) water, followed by adjustment of the solution pH with KOH until the solution pH was 6.49. The solution was then transferred into a 30 mL Teflon vessel, sealed in a steel autoclave, and heated in an oven at 240 °C for 48 h. Small plate-like crystals of the compound **UOHF-Zn** were obtained after cooling to room temperature at 5 °C/h with the final solution pH of 5.83. Upon washing with DI water and drying in air at ambient temperature, a yield of

https://doi.org/10.1021/acsomega.4c06188
ACS Omega 2024, 9, 38284−38294

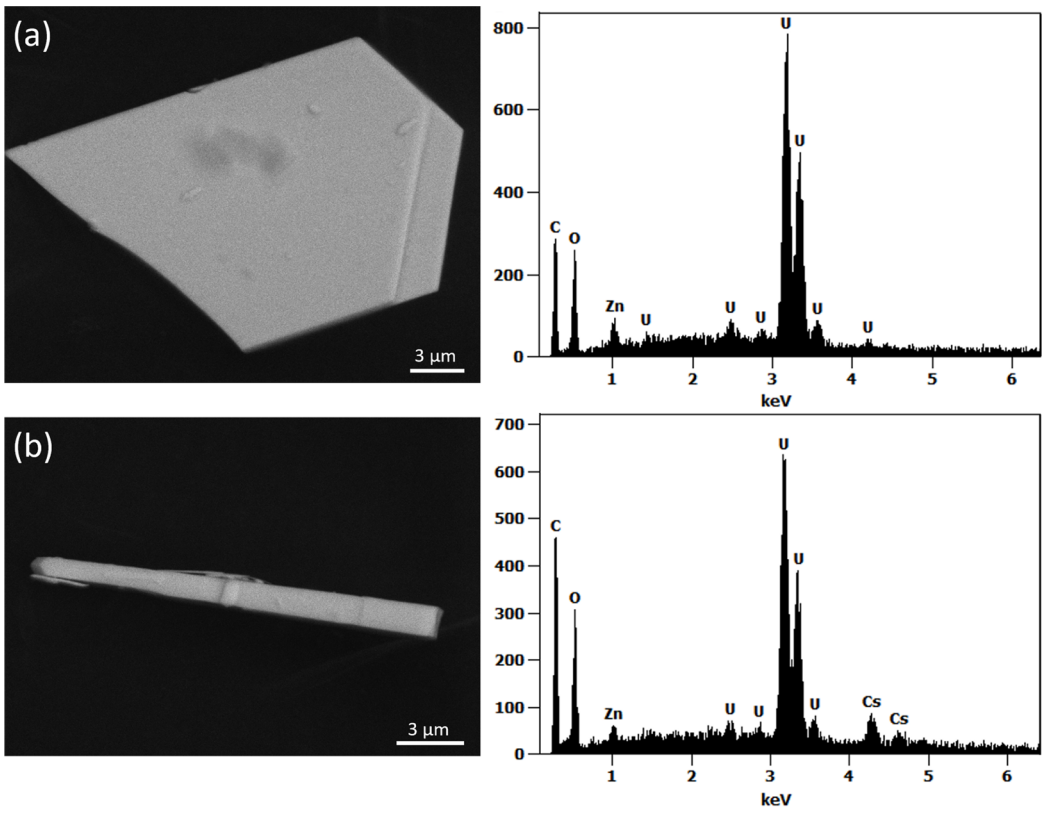

Figure 1. SEM analysis of **UOHF-Zn** (a) and **UOH-Zn** (b): backscattered SEM images of the crystals on the left and their corresponding EDS spectra on the right, confirming the presence of U and Zn (a) and U, Zn, and Cs (b) in the crystals.

~51 wt % (0.053 g) was isolated. Upon reaction completion, the reaction solution was still pale yellow in color, indicative of either unreacted uranium or water-soluble uranium byproducts also present in the final reaction solution. A decrease of the final solution pH to a pH range of 4 to 5.5 gave rise to a significant portion of amorphous powder and a very fine crystalline secondary phase, which was unable to be characterized further.

2.1.2. $Cs_2Zn(H_2O)_4[(UO_2)_4O_3(OH)_4]_2{\cdot}3H_2O$ (UOH-Zn). Zinc nitrate hexahydrate, $Zn(NO_3)_2{\cdot}6H_2O$ (0.0491 g, 0.165 mmol), and uranyl nitrate hexahydrate (0.0823 g, 0.165 mmol) were dissolved in 10 mL of deionized (DI) water, followed by adjustment of the solution pH with CsOH until the solution pH was 6.57. The solution was then transferred into a 30 mL Teflon vessel, sealed in a steel autoclave, and heated in an oven at 240 °C for 48 h. Small rod-like crystals of the compound **UOH-Zn** were obtained after cooling to room temperature at 5 °C/h with the final solution pH of 5.85. Upon washing with DI water and drying in air at ambient temperature, a yield of ~63 wt % (0.037 g) was isolated. Upon reaction completion, the reaction solution was still pale yellow in color, indicative of either unreacted uranium or water-soluble uranium byproducts also present in the final reaction solution. Adjustment of the final solution pH below 5.25 and above 6 gave rise to a major amorphous phase and a fine crystalline minor phase, which was unable to be characterized further.

2.2. Characterizations. *2.2.1. Synchrotron Single Crystal X-Ray Diffraction.* Suitable single crystals were harvested as either thin plates (**UOHF-Zn**: ~29 × 15 × 0.8 μm) or small needles (**UOH-Zn**: ~20 × 1.2 × 1.0 μm). Data collections for such challenging single crystals are not possible using a lab X-ray diffractometer, and as such, synchrotron X-ray diffraction was utilized.

The single crystal data for compounds **UOHF-Zn** (CCDC-2339546) and **UOH-Zn** (CCDC-2339545) were collected at 100(2) K on the MX2 beamline[42] at the Australian Synchrotron employing silicon double crystal monochromated synchrotron radiation (λ = 0.71079 Å). Data integration and reduction were undertaken with XDS.[43] Absorption corrections were applied to the data using SADABS.[44] The structures were solved by direct methods[45] and refined with SHELXL-2014[46] using the Olex2 graphical user interface.[47] All but hydrogen atoms were located on the electron density maps and refined anisotropically. The structure of **UOH-Zn** was refined using a two-component inversion twin with a Flack of 0.66(3). For the structure refinement of **UOHF-Zn**, one U atom (U5) has an abnormal elongated thermal ellipsoid, and all U atoms want to be lower than unity, likely due to the ineffective absorption corrections. In addition, some oxygen atoms also show small ellipsoids even with NDP (O18) likely due to the ineffective absorption corrections. Therefore, EADP was used to refine all of the oxygen atoms. The one-circle goniometer setup, a low beam attenuation applied to prevent crystal damage, and the poor diffraction at certain angles lead to the low data completeness and ineffective absorption corrections reflected as ripples around heavy U atoms.

2.2.2. Scanning Electron Microscopy (SEM). The crystal morphologies and elemental compositions were analyzed by using SEM coupled with energy dispersive spectrometry (EDS). Samples were carbon coated and examined in a Zeiss Ultra Plus scanning electron microscope (Carl Zeiss NTS GmbH, Oberkochen, Germany) operating at 15 kV equipped with an Oxford Instruments X-Max 80 mm^2 SDD X-ray

https://doi.org/10.1021/acsomega.4c06188
ACS Omega 2024, 9, 38284−38294

microanalysis system. EDS point analyses were carried out on relatively flat crystal surfaces with a Cu standard for calibration.

2.2.3. Raman Spectroscopy. Raman spectra were collected on a Renishaw inVia spectrometer equipped with a 785 nm excitation Ar laser from 2000 to 100 cm^{-1} with a spectral resolution of ~1.7 cm^{-1}.

2.2.4. Diffuse Reflectance Spectroscopy (DRS). Absorption spectra in the UV−visible region was recorded on an Agilent Cary 5000 spectrophotometer equipped with a Labsphere Biconical Accessory and referenced to a Labsphere certified standard.

2.2.5. Powder X-Ray Diffraction. Powder X-ray diffraction patterns were collected on a Bruker D8 Focus diffractometer equipped with Cu Kα (λ = 1.5418 Å) radiation in the angle range of 5−90° 2θ with a step size of 0.02° (2θ) and a data collection time of 3 s per step. The collected data were fit to their respective phases via the Le Bail method using TOPAS.[48]

3. RESULTS AND DISCUSSION

3.1. Material Synthesis and Microstructure Investigation. Crystals of **UOHF-Zn** and **UOH-Zn** were successfully isolated after synthesis under hydrothermal conditions with uranyl and zinc nitrates as the metal sources. Prior to heating, adjustment of the pH to 6.49 was performed using KOH for **UOHF-Zn**, with a final solution pH of 5.83 obtained after synthesis. The hydroxide source was changed to CsOH for **UOH-Zn**, wherein the starting solution pH was adjusted to 6.57, resulting in a final solution pH of 5.85. The choice of pH was driven by recent successes in incorporating 2+ secondary cations at higher pH values,[32,38] with further consideration also that, upon addition of more of the hydroxide, there would also be increased proportions of K^+ and Cs^+ in solution. Of note also is that the change in reaction volume between the two syntheses results in slight changes in both reactant concentrations and reaction pressures. Previous studies reveal that a larger reaction volume may impart a level of influence on the formation of a layered-type structure over that of a framework.[34,49]

SEM-EDS analysis (Figure 1a) revealed a plate-like crystal morphology for **UOHF-Zn**, with EDS analysis confirming the successful incorporation of U and Zn in an atomic ratio of 5.5:1. Notable was the absence of any K in the structure. Upon examination of **UOH-Zn** with SEM (Figure 1b), a distinctly different crystal morphology was identified, with needle-like crystals instead observed. EDS analysis revealed that both Zn and Cs had been successfully incorporated into the structure, with a U/Zn/Cs ratio of 8:1:2. Interestingly, the atomic ratios closely matched that of a published UOH-Mg compound, wherein crystals containing a U/Mg/Na ratio of 8:1:2 were obtained in similar needle-like crystals.[38]

In both syntheses, a similar minor phase consisting of hexagonal plate crystals was also identified (Figure S1), with EDS analysis confirming that the material only contained U and O, with no secondary cations present. Thus, this minor phase was not explored further. Separation of this minor phase was performed, following which powder X-ray diffraction was performed to establish that the bulk material was phase pure and matched the calculated pattern obtained from single-crystal data. A Le Bail fitting was performed and revealed that **UOHF-Zn** (Figure S2, top) showed a close match between the bulk phase and the calculated pattern, confirming a phase pure compound was obtained for further analysis. Analysis of **UOH-Zn** (Figure S2, bottom) revealed that a slight impurity was present in the bulk material, best evidenced by additional peaks between 25° and 35° 2θ. Given the presence of the minor phase under SEM, this was not unexpected, and it was confirmed that the major phase present closely matched that determined from the single-crystal data and was suitable for further analysis.

3.2. Crystal Structures and Discussion. Crystals of suitable quality were isolated for both **UOHF-Zn** and **UOH-Zn**, and single-crystal X-ray diffraction data were obtained by using synchrotron radiation. The crystal data and structure refinement details for **UOHF-Zn** and **UOH-Zn** are summarized in Table 2, with selected bond lengths (Å) and angles (°) provided in Tables 3 and 4, respectively.

Table 2. Crystal Data and Structure Refinement Details for Compounds UOHF-Zn and UOH-Zn

compound	UOHF-Zn	UOH-Zn
CCDC	2339546	2339545
empirical formula	$ZnO_{22}U_{5.5}$	$Cs_2ZnO_{37}U_8$
formula weight	1726.54	2827.43
crystal system	triclinic	orthorhombic
space group	$P\bar{1}$	$Cmc2_1$
a (Å)	8.2010(16)	14.979(3)
b (Å)	10.951(2)	13.885(3)
c (Å)	11.510(2)	16.577(3)
α (deg)	111.40(3)	90
β (deg)	102.35(3)	90
γ (deg)	104.24(3)	90
volume (Å^3)	878.5(4)	3447.9(12)
Z/μ (mm^{-1})	2/51.958	4/40.306
min/max θ (deg)	2.018/24.995	2.347/25.000
d_{calcd} (g cm^{-3})	6.527	5.447
GOF	1.138	1.049
final R_1[a] [$I > 2\sigma(I)$]	0.0527	0.0513
final wR_2[b] [$I > 2\sigma(I)$]	0.1559	0.1135
Flack	-	0.66(3)

[a] $R_1 = \Sigma||F_o| - |F_c||/|F_o|$. [b] $wR_2 = \{\Sigma[w(F_o^2 - F_c^2)^2]/\Sigma[w(F_o^2)^2]\}^{1/2}$.

UOHF-Zn was identified as crystallizing in the triclinic $P\bar{1}$ space group with six distinct uranium centers and two zinc centers, each in partial occupancies, composing the asymmetric unit. Extending the structure gives rise to a framework-type structure, with the uranium centers composing the framework backbone and the Zn centers lying in the channels. The uranium sites within the framework take on two distinct geometries, U3 and U5 present in octahedral geometries and the remaining U centers existing as pentagonal bipyramids. The two zinc centers are also in different geometries, with Zn1 having a 6-fold, distorted octahedral geometry and Zn2 taking on a 5-coordinate trigonal bipyramidal orientation.

The layout of the uranyl polyhedra sheets is structurally similar to that of β-U_3O_8 and those seen in previous UOH/F systems,[33−35] with chains of U2, U4, and U6 pentagonal bipyramids connected via O−O edge sharing and U3 and U5 octahedra linking the chains together (Figure 2b). The layers are pillared through pairs of U1−U1 units, giving rise to the channels that extend throughout the framework structure. The two octahedral U centers show quite interesting coordination environments, differing significantly from each other. U3 resembles that of a uranyl unit, with four equatorial U−O bonds between 2.174(18) and 2.214(19) Å and two shorter axial bonds of 1.849(18) − 1.948(19) Å in length. The slightly

https://doi.org/10.1021/acsomega.4c06188
ACS Omega 2024, 9, 38284−38294

Table 3. Selected Bond Lengths (Å) and Angles (°) for UOHF-Zn

UOHF-Zn							
U1−O1	1.794(18)	U2−O3	1.930(18)	U3−O5[a]	2.194(18)	U4−O8	2.263(18)
U1−O2	1.768(18)	U2−O4	1.827(19)	U3−O6	1.849(18)	U4−O8[b]	2.249(19)
U1−O3	2.396(18)	U2−O5[c]	2.279(19)	U3−O7	1.948(19)	U4−O9	2.271(19)
U1−O7[d]	2.344(18)	U2−O5	2.263(18)	U3−O8	2.214(19)	U4−O10	1.838(18)
U1−O11[d]	2.386(18)	U2−O13[a]	2.267(18)	U3−O9	2.174(18)	U4−O11	1.998(18)
U1−O11[a]	2.495(18)	U2−O14[e]	2.421(19)	U3−O18[f]	2.182(19)	U4−O12	2.432(18)
U1−O13[a]	2.354(18)	U2−O18[f]	2.312(18)	O6═U3═O7	174.3(8)	U4−O13	2.161(18)
O2═U1═O1	179.2(9)	O4═U2═O3	176.4(8)			O10═U4═O11	173.9(8)
U5−O12[g]	1.978(18)	U6−O9[h]	2.268(18)	Zn1−O1[a]	2.210(19)	Zn2−O4	2.08(2)
U5−O12	1.978(18)	U6−O12[h]	2.467(19)	Zn1−O6	2.022(19)	Zn2−O16[i]	2.00(2)
U5−O14[g]	1.966(19)	U6−O14[h]	2.468(18)	Zn1−O17	2.010(19)	Zn2−O21	1.89(2)
U5−O14	1.966(19)	U6−O16	1.848(18)	Zn1−O20	1.983(19)	Zn2−O22	2.02(2)
U5−O15[g]	2.298(18)	U6−O17	1.861(18)	Zn1−O21	1.974(19)	Zn2−O23	2.01(4)
U5−O15	2.298(18)	U6−O18[b]	2.282(19)	Zn1−O21[f]	2.33(2)		
O12═U5═O12	180.0(7)	U6−O19	2.1685(10)				
		O16═U6═O17	176.1(8)				

[a]X, Y, −1 + Z. [b]1 − X, 1 − Y, 1 − Z. [c]1 − X, 2 − Y, 1 − Z. [d]−X, 2 − Y, 1 − Z. [e]−X, 1 − Y, 1 − Z. [f]1 − X, 1 − Y, 1 − Z. [g]−X, 1 − Y, 2 − Z. [h]1 + X, Y, Z. [i]2 − X, 1 − Y, 1 − Z.

Table 4. Selected bond lengths (Å) and angles (deg) for UOH-Zn

UOH-Zn							
U1−O1	1.79(2)	U2−O3[a]	2.45(2)	U3−O5	2.43(2)	U4−O3[b]	2.52(2)
U1−O2	1.77(2)	U2−O5	2.52(2)	U3−O6[b]	2.26(2)	U4−O4	2.27(2)
U1−O3	2.41(2)	U2−O6	2.27(3)	U3−O9[b]	2.51(3)	U4−O9[c]	2.40(2)
U1−O4	2.35(2)	U2−O7	1.82(3)	U3−O10	2.27(2)	U4−O10[d]	2.27(2)
U1−O5	2.44(2)	U2−O8	1.84(3)	U3−O11	1.80(3)	U4−O13	2.44(2)
U1−O6	2.22(2)	U2−O9	2.36(2)	U3−O12	1.81(3)	U4−O14	1.77(3)
U1−O13[e]	2.59(2)	U2−O10	2.23(2)	U3−O13	2.47(2)	U4−O15	1.79(3)
O2═U1═O1	178.7(11)	O7═U2═O8	177.8(11)	O11═U3═O12	176.3(11)	O14═U4═O15	177.5(11)
Cs1−O2[f]	3.12(2)	Cs1−O11[e]	3.15(3)	Cs2−O8[d]	3.19(2)	Zn1−O1	2.19(2)
Cs1−O2	3.12(2)	Cs1−O11[g]	3.15(3)	Cs2−O8[h]	3.19(2)	Zn1−O7	2.05(3)
Cs1−O6	3.43(3)	Cs1−O16[g]	3.31(3)	Cs2−O10[d]	3.22(3)	Zn1−O11	2.23(2)
Cs1−O6[f]	3.43(3)	Cs1−O17[g]	3.13(3)	Cs2−O10[h]	3.22(3)	Zn1−O16	2.19(3)
Cs1−O8[f]	3.23(2)	Cs1−O19	3.74(4)	Cs2−O12[h]	3.33(2)	Zn1−O17	2.11(2)
Cs1−O8	3.23(2)			Cs2−O12[d]	3.33(2)	Zn1−O18	2.06(2)
				Cs2−O14[i]	3.13(2)		
				Cs2−O14	3.13(2)		

[a]X, −Y + 1, Z − 1/2. [b]−X + 3/2, Y − 1/2, Z. [c]X, −Y + 1, Z + 1/2. [d]−X + 3/2, −Y + 1/2, Z + 1/2. [e]−X + 3/2, Y + 1/2, Z. [f]−X + 3/2, −Y + 1/2, Z + 1/2. [g]X + 1/2, Y + 1/2, Z. [h]X − 1/2, −Y + 1/2, Z + 1/2. [i]−X + 1, Y, Z.

elongated U3−O7 bond arises from the additional coordination of O7 to U1, with this type of cation−cation interaction (CCI) reported to result in a slight elongation of the uranyl bond.[50]

In comparison, U5 lacks the appearance of a uranyl bond. U5 lies coplanar with O12 and O14, with observed bond lengths of 1.978(18) and 1.966(19) Å, respectively, and O12−U5−O12 and O14−U5−O14 bond angles of 180°. The O12−U5−O14 angles are 82.1(8)° and 97.9(8)°, with this uranium center very closely matching a structure reported by Burns and coworkers.[50] U5 donates double CCIs through both the O12 and the O14 oxygens to neighboring pentagonal bipyramidal uranium centers, with bond lengths of 1.978(18) and 1.966(19) Å matching those expected for such interactions. As such, the U5 site can be defined as having a tetraoxido core. Such uranium centers have also been found in other synthetic systems which have the same β-U_3O_8 layer topology; however, in such cases, further discussion of the coordination environment was not mentioned.[32,38,40] Excluding U5, the remaining uranium centers have bond length and angle values that are consistent with previously reported UOHF materials, including the slight bending of the typically linear uranyl bonds.[29,32,33,35]

Examining the bond valence sum (BVS) calculations (Table S1), using values obtained from the literature,[14] confirmed that all U centers are present as U^{6+} [U1 (5.96), U2 (5.87), U3 (5.75), U4 (5.91), U5 (5.90), and U6 (5.91)], with Zn^{2+} [Zn1 (2.19) and Zn2 (2.20)] also confirmed for the Zn centers. The majority of the oxygens are present as O (O1−O14, O16−O18) with one OH (O21) and three full occupancy (O15, O20, and O22) and two half occupancy (O19 and O23) H_2O species, allowing for the formulation of **UOHF-Zn** to be determined as $Zn_2(OH)_2(H_2O)_5[(UO_2)_{10}UO_{14}(H_2O)_3]$ (Z = 2).

While the uranyl framework is comparable to other UOHF structures, of particular interest, however, is the nature of the Zn^{2+} cations that lie in the channels. **UOHF-Zn** is the first reported UOHF structure incorporating transition metal ions alone, and only the third with solely 2+ cations,[27,29] and thus

https://doi.org/10.1021/acsomega.4c06188
ACS Omega 2024, 9, 38284−38294

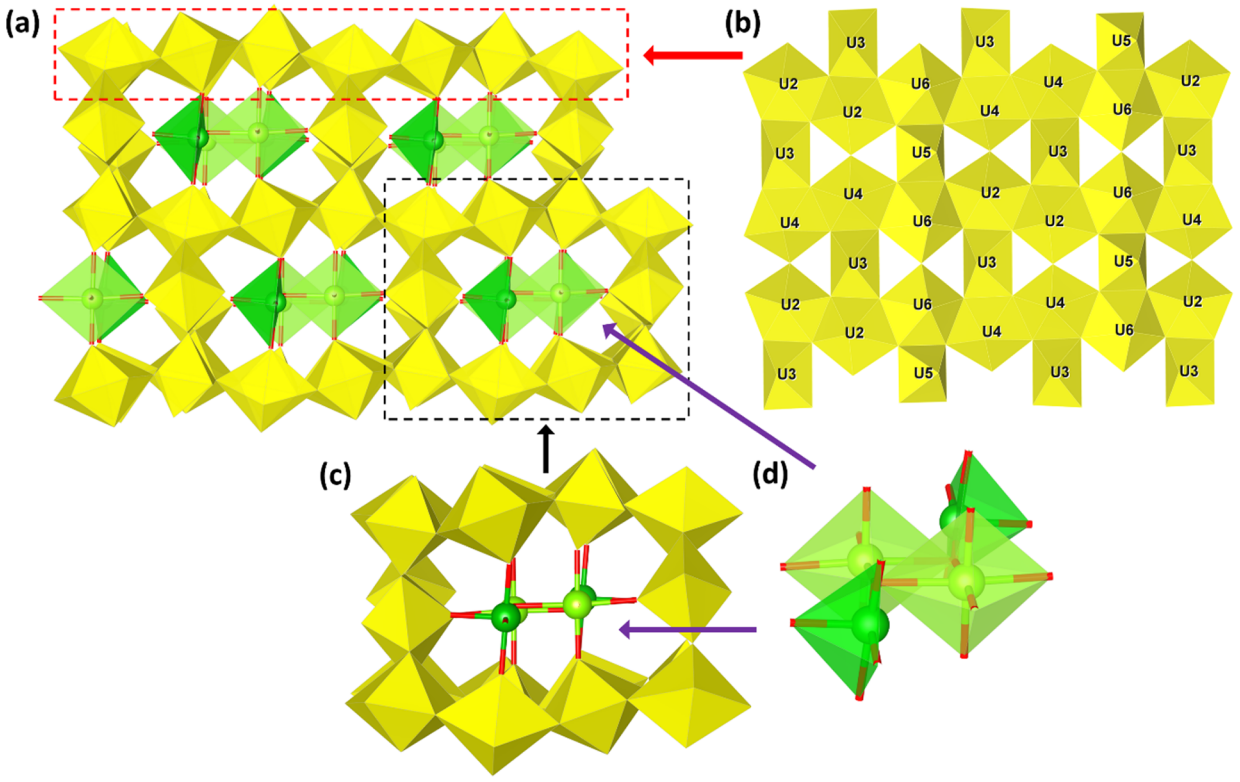

Figure 2. Crystal structure of **UOHF-Zn**: a polyhedral crystal structure along the *c*-axis (a), a polyhedral view of the uranyl oxide hydroxide layer with a β-U_3O_8 topology (b), and the 5- and 6-fold coordinated Zn^{2+} centers composing the Zn binding unit and lying within the channels of the framework (c) and (d); U in yellow, 6-fold Zn in dark green, and 5-fold Zn in pale green.

their coordination environment is intriguing to explore. Also of note is that the reported space group, that of $P\bar{1}$, has only been reported once previously for a UOHF compound.[33] Upon examination of the zinc centers, immediately evident is that the Zn^{2+} cations form discrete units that are isolated from one another, each composed of two Zn1 and two Zn2 centers (Figure 2d). Two Zn1 moieties make up the center of this unit, connected through the O−O edge sharing (O21), with the two Zn2 centers projecting into the channels and linked via corner sharing through the O21. These Zn units are comparable to the binding motif seen for UOHF-Er/Y,[33] wherein the interchannel cations exist isolated from their neighboring cations, as opposed to forming chains that extend along the channels of the framework as seen in other UOHF structures.[34,35] Given that the $P\bar{1}$ space group found for **UOHF-Zn** is the same as that reported in the UOHF-Er/Y study, this similarity is logical. In contrast to that study, however, is the existence of a Zn binding unit in **UOHF-Zn** in place of the singular Er/Y^{3+} cation. The most likely explanation for this notable difference is the ionic radii of Zn^{2+} (0.68−0.74 Å), which is markedly smaller than that of Er/Y^{3+} (1.004 Å).[51] Thus, it makes sense that to bind within channels with comparable dimensions, a different binding motif must be adopted. Related to this consideration is coordination between the Zn unit and the uranyl framework. While each of the Zn centers is coordinated to the uranyl polyhedra layers through the axial U−O bonds, Zn1 also coordinates to the U1 pentagonal bipyramids making up the "walls" of the channels through the axial oxygens (O1), anchoring the Zn unit to all four sides of the framework (Figure 2c), a unique feature heretofore unseen in any UOHF structure. A second aspect that may also drive the observed changes in structure from those previously reported, likely in tandem with the change in ionic radius, is the 2+ charge on the Zn centers. However, these structural features are also unique compared to those seen for Cd^{2+}, Pb^{2+}, and Sr^{2+},[27,29,32] which are each significantly larger in ionic radius compared to Zn^{2+}.

In comparison to the previously reported UOHF-Cd structure,[32] K^+ is notably absent in **UOHF-Zn** despite comparable synthetic conditions being used in both syntheses. The smaller ionic radius of Zn^{2+} is again likely to have played a role in this result, providing additional freedom for the secondary cation to be incorporated and satisfying the charge balance of the structure without the need for K^+ to also being present. Previously hypothesized,[19,32] and clearly highlighted by **UOHF-Zn**, is the fact that the ionic radius of the secondary cation is a critical aspect to consider when examining these materials.

Examining the crystal structure of **UOH-Zn** revealed that it crystallized in the orthorhombic space group $Cmc2_1$. Confirming the results found with SEM-EDS (Figure 1b), the asymmetric unit was found to contain two half occupancy Cs centers along with one-half occupancy Zn site and four full occupancy U centers, confirming the elemental ratio of 2:1:8. All four U sites take on the same pentagonal bipyramidal geometry, with the Zn existing in a distorted octahedral geometry. The two Cs sites differ significantly, with an 11-coordinate all faced capped trigonal prism (Cs1) and an 8-fold distorted bicapped trigonal prismatic (Cs2) both linked through O−O edge sharing. In contrast to **UOHF-Zn**, the uranium oxide hydroxide layer instead more closely resembled that of schoepite (Figure 3d).[52] Chains of −U3−U2− centers are linked through the U1 and U4 centers via the O−O edge and corner sharing, with the axial oxygens projecting above and

https://doi.org/10.1021/acsomega.4c06188
ACS Omega 2024, 9, 38284−38294

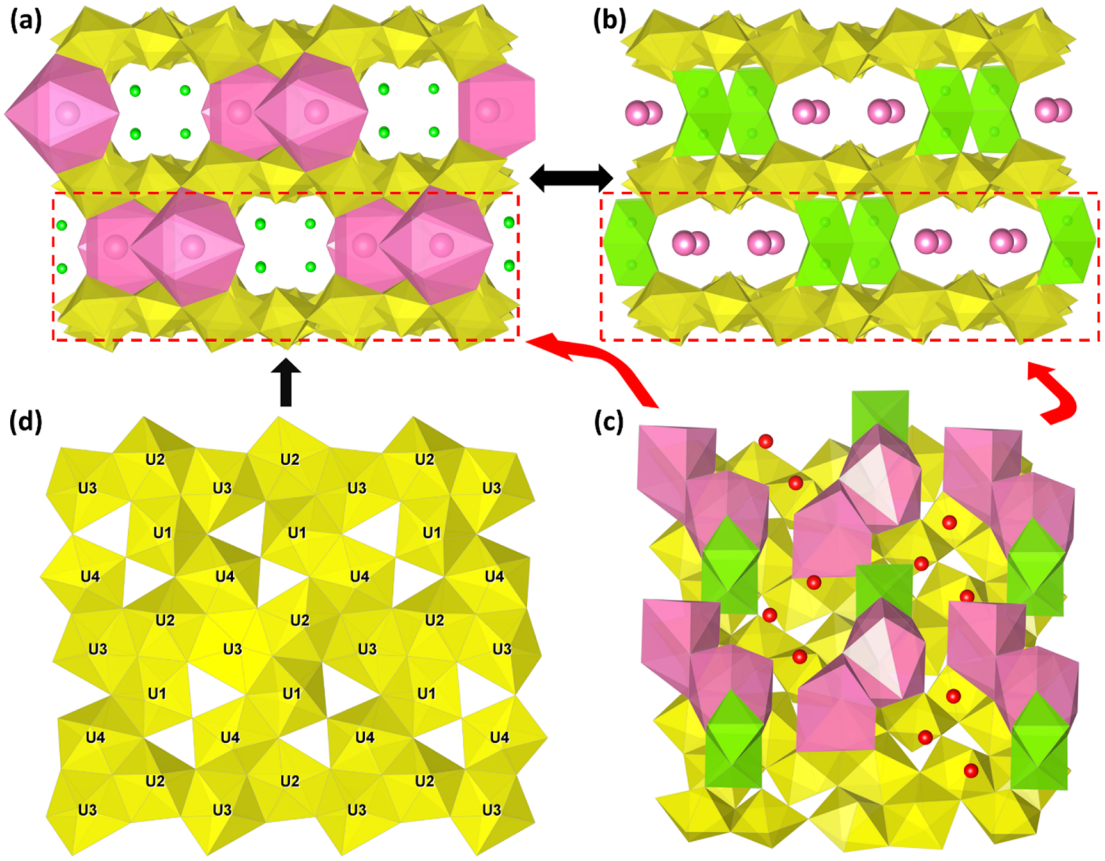

Figure 3. Crystal structure of **UOH-Zn**: a polyhedral crystal structure along the *c*-axis with Zn^{2+} shown as balls (a), a polyhedral crystal structure along the *c*-axis with Cs^{+} shown as balls (b), a polyhedral view illustrating the Cs−Zn "pillars" and H_2O molecules along the *b*-axis (c), and a polyhedral view of the uranyl oxide hydroxide layer with a schoepite-like layer topology (d); U in yellow, Cs in pink, and Zn in green.

below the layer and participating in the uranyl−cation interactions.

The coordination sphere about each of the U sites shows the expected uranyl bonds in the axial positions (1.77(2)−1.84(3) Å), with slightly distorted U═U═O uranyl bond angles of 176.3(11)°−178.7(11)°. The equatorial U−O bonds fall in the range of 2.22(2)−2.59(2) Å, consistent with the uranyl centers in previously reported structures.[28,30,39] Each of these uranyl polyhedra layers are separated by a distance of ∼6.8 Å, within which lie the secondary cations. The BVS calculations (Table S2) confirmed that all U centers are present in the U^{6+} state [U1 (5.98), U2 (5.85), U3 (5.88), and U4 (6.07)], with the Cs centers existing as Cs^{+} [Cs1 (1.19) and Cs2 (0.94)] and the Zn center as Zn^{2+} (1.86). Four OH (O3, O4, O5, and O13), four half occupancy H_2O (O16, O17, O19 and O20), and three half occupancy unbound H_2O molecules (O20−O22) are all present, and thus **UOH-Zn** was formulated as $Cs_2Zn(H_2O)_4[(UO_2)_4O_3(OH)_4]_2{\cdot}3H_2O$ (Z = 4).

Of immediate interest when examining the interlayer cations is the dual-cation system, as monovalent cations have been identified as an additional means of providing a charge balance to the uranium oxide hydroxide layer. As such, introducing alkali metals that will be present in the surroundings of SNF in a deep geological setting, such as Na^{+}, K^{+} and Cs^{+}, may provide further insight into the stability and flexibility of the alteration products of uranyl species. Notably, the presence of both Cs^{+} and Zn^{2+} in the interlayer of **UOH-Zn** is the first reported UOH material with Cs^{+} present in a dual-cation system. The binding of these cations is comparable to that of Zn^{2+} in **UOHF-Zn** in that the Cs^{+} and Zn^{2+} form isolated binding units, in this case consisting of one center each of Cs1 and Cs2, along with two Zn2 centers (Figure 3b). The two Zn centers coordinate each other and Cs1 through O−O edge sharing, accounting for the increased coordination number for Cs1 compared to Cs2. These binding units are then bound to each uranyl layer again through uranyl−cation interactions. The result is isolated Cs−Zn "pillars", with void space lying between each and giving rise to a pseudoframework structure. Within these voids can be found one bound (O19) and three unbound (O20−O22) water molecules (Figure 3b). This pseudoframework is comparable to structures published by Zhang et al.[49] and Rivenet et al.;[40] however, a notable difference is that in each of those studies, the "pillar" consisted of a singular ion, where in **UOH-Zn**, the pillar is made up of the Cs−Zn binding unit.

An interesting comparison can also be made to another recent study by Zhang et al.[38] In that study, a dual-cation interlayer of Na^{+} and Mg^{2+} was reported, termed **UOH-Mg2n**, and was found to have an identical atomic ratio of 2:1:8 (Na/Mg/U), with the same molecular formula as that reported for **UOH-Zn**. Notably different, however, was that **UOH-Mg2n** crystallized in the $P\bar{1}$ space group and was found to have a novel uranium oxide hydroxide layer compared to the schoepite-like topology reported for **UOH-Zn**. In examining the two materials, what is apparent is both the near identical ionic radii of Mg^{2+} and Zn^{2+} (0.72−0.74 Å) and the increased ionic radius of Cs^{+} compared to Na^{+} (1.67−1.88 Å vs 1.02−1.39 Å).[51] While additional factors must also be considered,

https://doi.org/10.1021/acsomega.4c06188
ACS Omega 2024, 9, 38284−38294

such as the influence of the solution pH and the binding nature of the other cation species (being Mg^{2+} and Zn^{2+}), what these two studies further emphasize is the intricate balance of all components within the synthesis of these materials, and as such, the multifaceted nature of the alteration of uranium oxide materials when placed within a geological repository.

3.3. Electronic Structures. The calculated BVS values for both materials (Tables S1 and S2) indicate that only U^{6+} is present, unlike previously reported UOH/F structures.[27,33,53] The dominating feature of both DR spectra (Figure 4) is the

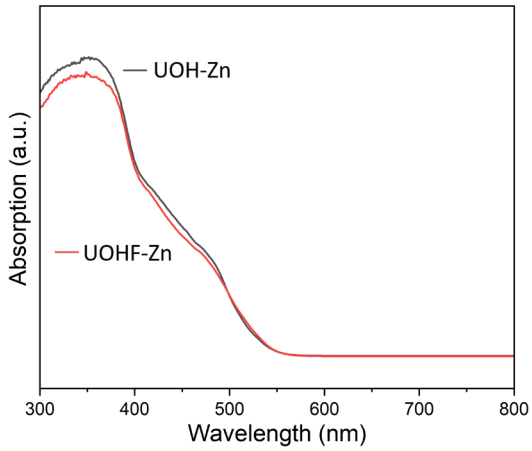

Figure 4. DR spectra of **UOHF-Zn** (red) and **UOH-Zn** (gray) in the UV−vis region.

broad absorption peaks in the UV region (300−500 nm), with peaks at ∼350 nm and a possible obscured peak at ∼460 nm, as indicated by a shoulder, arising from charge-transfer bands from the U^{6+} centers.

3.4. Vibrational Modes. Raman spectroscopy was employed to explore the vibrational modes of **UOHF-Zn** and **UOH-Zn**. The spectra for both materials are comparable (Figure 5), expected given the similar nature of their uranium

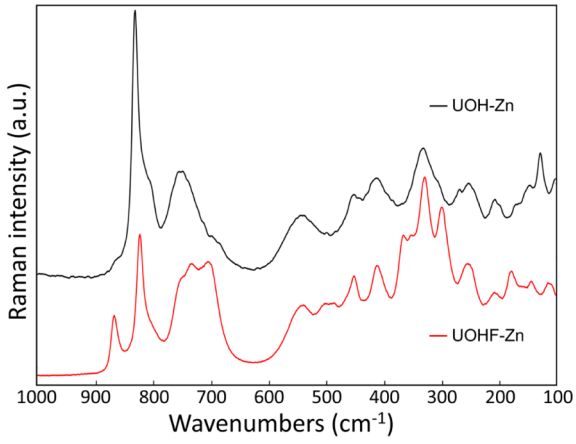

Figure 5. Raman spectra of **UOHF-Zn** (red) and **UOH-Zn** (black).

oxide hydroxide layers. Peaks in the region of 900−650 cm^{-1} can be assigned to $\nu_1(UO_2)^{2+}$ vibrations corresponding to the uranyl U═O bonds. Given the variety of unique U centers and the U═O bond lengths spanning a broad range (1.768−1.98 Å), multiple $\nu_1(UO_2)^{2+}$ vibrations are evident in both spectra. Additional peaks at 865 and 700 cm^{-1} are evident in the **UOHF-Zn** spectrum, expected given the two additional 6-fold U(VI) centers. These values are broadly consistent with the values reported for U═O bonds in the literature.[54,55]

The broad, medium intensity peaks between 580 and 320 cm^{-1} arise from $\gamma[U_3(OH)_3]$ bending vibrations, $\nu(U_3O)$ bridge elongations, and $\nu(U-O_{ligand})$ vibrations, with the remaining peaks assigned to $\nu_2(UO_2)^{2+}$ bending vibrations (295−200 cm^{-1}) and lattice vibrations (180−100 cm^{-1}).

3.5. Implications and Perspectives. The capacity to synthesize two novel UOH/F materials under similar reaction conditions, with only variations on the concentrations and identity of the cation species, clearly demonstrates the value of synthetic UOH compounds in identifying and studying the possible alteration products of uranium oxides in a geological setting. The abundance of transition metals in the Earth's crust guarantees that these species will be present in the surroundings of any deep geological repository, yet due to paragenesis, no such UOH minerals are available for study, driving the need to make such phases synthetically. However, the lack of reported UOH materials containing transition metals[28,32,40,41] makes understanding the influence of 3d/4d transition metals on the alteration pathway of uranium oxides challenging. In successfully incorporating a small 3d transition metal into a UOHF structure, the scope of what elements may adopt this phase along the alteration pathway is significantly broadened, highlighting the complexity of these systems. The novel binding motif adopted by the Zn^{2+} cations in the channels of the framework, again governed by the smaller ionic radius compared to cations previously reported, provides critical insight into the possible options available to meet both the essential size and charge balance required to be incorporated into these materials.

With only a few examples of synthetic UOH structures containing multiple interlayer cation species, despite the much larger number of UOH minerals containing such systems, there is a clear gap in knowledge that must be filled. Through the successful incorporation of both Zn^{2+} and Cs^{+} cations into a layered UOH structure, the first time Cs^{+} has been incorporated alongside a second cation species in such a material, this knowledge gap is clearly exemplified. The abundance of Cs in SNF, along with the abundance of Na and K in the surroundings of any geological repositories, makes understanding these systems better a clear priority. Also highlighted within this work was the exclusion of K^{+} from the UOHF structure despite comparable reaction conditions. The additional factors of reactant concentration and reaction pressure were also considered via the adjustment of the total reaction volume. However, in comparing both **UOHF-Zn** and **UOH-Zn** to similar structures in the literature,[32,38] which, while having very similar reaction conditions, have drastically different crystal structures, we can elucidate that the predominant driving force behind such changes is very likely to be that of the ionic radii of the secondary cation species.

Invaluable also is the means by which these materials are examined crystallographically. In isolating crystals of synthetic UOH phases containing either Zn^{2+} or Zn^{2+} and Cs^{+} cations, it was possible to explore the subtle differences in their crystal structures compared to others previously reported. Highlighting the value of this is the comparison between the herein reported Zn^{2+}/Cs^{+} layered UOH structure to that of a published UOH with Mg^{2+}/Na^{+} ions, which despite having identical atomic ratios and chemical formulas, had distinct differences in their respective crystal structures that may have

https://doi.org/10.1021/acsomega.4c06188
ACS Omega 2024, 9, 38284−38294

otherwise remained unobserved. Further work toward growing and isolating crystals of high enough quality to obtain single crystal X-ray data is therefore critical to gaining a deeper understanding into these materials.

4. CONCLUSIONS

Two novel UOH/F materials containing Zn^{2+} or Zn^{2+} and Cs^{+} have been successfully synthesized hydrothermally with solution pH controlled through the addition of dilute solutions of KOH and CsOH, respectively. The first of the two structures, **UOHF-Zn**, is a framework-type structure and crystallized in the $P\bar{1}$ space group, with Zn^{2+} cations lying within the channels. This is the first example of small 3d transition metals being successfully incorporated into a UOHF material with the ionic radius of the Zn^{2+} ion significantly smaller than any previously reported inside a framework-type compound. The second structure, **UOH-Zn**, was solved in the $Cmc2_1$ space group and consisted of schoepite-like UOH layers with Cs^{+} and Zn^{2+} cations making up the interlayer cations with a U/Zn/Cs ratio of 8:1:2. The schoepite-like UOH layer differed from that observed for **UOHF-Zn**, which instead had a uranium oxide hydroxide layer resembling that of β-U_3O_8. Interestingly, the Zn^{2+} and Cs^{+} cations formed novel "pillars", which separated the uranyl layers and resulted in a pseudoframework structure, with both bound and unbound water lying in the framework voids. Unfortunately, removal of these waters has previously been found to result in a loss of crystallinity, indicative of a complete collapse of the structure.[56] As such, these voids were unable to be accessed for additional study, as any removal of either the cocoordinated or solvent water molecules during the activation and degassing processes for gas absorption would result in structural collapse.

Also of note was the dual-cation system and the first time that Cs^{+} has been successfully incorporated alongside a second cation in such materials.

Significantly, the differences between the two structures despite the synthetic conditions closely resembling one another, except for the identity of the base and the reaction volume, highlight the sensitivity of these materials to their immediate environment during formation. Additionally, the ionic radii of the cations being incorporated within these structures were highlighted as playing a critical role in driving the formation and alteration of these UOH/F systems. From this study, further research is therefore warranted to explore the capability of 3d transition metals to be incorporated into these systems, with additional studies exploring the effect of dual-cation systems on the final product also needed to better understand the chemistry driving the formation of these materials.

■ ASSOCIATED CONTENT

Supporting Information

The Supporting Information is available free of charge at https://pubs.acs.org/doi/10.1021/acsomega.4c06188.

SEM-EDS data; PXRD data; BVS calculations (PDF)
CCDC-2339546 (**UOHF-Zn**) (CIF)
CCDC-2339545 (**UOH-Zn**) (CIF)

■ AUTHOR INFORMATION

Corresponding Author

Timothy A. Ablott − *Australian Nuclear Science and Technology Organisation, Kirrawee, New South Wales 2232, Australia*; orcid.org/0000-0002-6611-9050; Email: ablottt@ansto.gov.au

Authors

Kimbal T. Lu − *Australian Nuclear Science and Technology Organisation, Kirrawee, New South Wales 2232, Australia*

Yingjie Zhang − *Australian Nuclear Science and Technology Organisation, Kirrawee, New South Wales 2232, Australia*

Complete contact information is available at: https://pubs.acs.org/10.1021/acsomega.4c06188

Author Contributions

The manuscript was written through contributions of all authors. All authors have given approval to the final version of the manuscript.

Notes

The authors declare no competing financial interest.

■ ACKNOWLEDGMENTS

We would like to thank I. Karatchevtseva for Raman measurement, the Nuclear Science and Technology (NST), ANSTO, for synthesis and characterization of materials. The crystallographic data for compounds **UOHF-Zn** and **UOH-Zn** were collected on the MX2 beamline at the Australian Synchrotron, a part of ANSTO, and made use of the Australian Cancer Research Foundation (ACRF) detector.

■ ABBREVIATIONS

BVS, bond valence sum; DR, diffuse reflectance; EDS, energy dispersive spectrometry; SEM, scanning electron microscopy; SNF, spent nuclear fuel; UOH, uranium oxide hydrate; UOHF, uranium oxide hydrate framework

■ REFERENCES

(1) Mathew, M. D. Nuclear energy: A pathway towards mitigation of global warming. *Prog. Nucl. Energy* **2022**, *143*, 104080.
(2) Alyokhina, S. Thermal analysis of certain accident conditions of dry spent nuclear fuel storage. *Nucl. Eng. Technol.* **2018**, *50* (5), 717−723.
(3) Zhang, Y.; Kong, L.; Ionescu, M.; Gregg, D. J. Current advances on titanate glass-ceramic composite materials as waste forms for actinide immobilization: A technical review. *J. Eur. Ceram. Soc.* **2022**, *42* (5), 1852−1876.
(4) Mallants, D.; Travis, K.; Chapman, N.; Brady, P. V.; Griffiths, H. The State of the Science and Technology in Deep Borehole Disposal of Nuclear Waste. *Energies* **2020**, *13* (4), 833.
(5) Paulillo, A.; Dodds, J. M.; Milliken, A.; Palethorpe, S. J.; Lettieri, P. The environmental impacts of reprocessing used nuclear fuels: A UK case study. *Sustainable Mater. Technol.* **2020**, *25*, No. e00186.
(6) Ewing, R. C. Long-term storage of spent nuclear fuel. *Nat. Mater.* **2015**, *14* (3), 252−257.
(7) Janeczek, J.; Ewing, R. C. Dissolution and alteration of uraninite under reducing conditions. *J. Nucl. Mater.* **1992**, *190* (C), 157−173.
(8) Janeczek, J.; Ewing, R. C. Structural formula of uraninite. *J. Nucl. Mater.* **1992**, *190* (C), 128−132.
(9) Wronkiewicz, D. J.; Bates, J. K.; Wolf, S. F.; Buck, E. C. Ten-year results from unsaturated drip tests with UO_2 at 90°C: Implications for the corrosion of spent nuclear fuel. *J. Nucl. Mater.* **1996**, *238* (1), 78−95.
(10) Finch, R. J.; Ewing, R. C. The corrosion of uraninite under oxidizing conditions. *J. Nucl. Mater.* **1992**, *190*, 133−156.
(11) Plasil, J. Oxidation-hydration weathering of uraninite: The current state-of-knowledge. *J. Geosci.* **2014**, *59* (2), 99−114.

(12) Plásil, J. Uranyl-oxide hydroxy-hydrate minerals: Their structural complexity and evolution trends. *Eur. J. Mineral.* **2018**, *30* (2), 237−251.
(13) Burns, P. C. Crystal chemistry of uranium oxocompounds: An overview. In *Structural Chemistry of Inorganic Actinide Compounds*, Krivovichev, S. V.; Burns, P. C.; Tananaev, I. G., Eds.; Elsevier, 2007; pp. 130. DOI: .
(14) Burns, P. C.; Ewing, R. C.; Hawthorne, F. C. The crystal chemistry of hexavalent uranium; polyhedron geometries, bond-valence parameters, and polymerization of polyhedra. *Can. Mineral.* **1997**, *35* (6), 1551−1570.
(15) Burns, P. C.; Konings, R. J. M.; Stoller, R. E. Hydrated Uranium Oxides, In *Comprehensive Nuclear Materials*, 2nd ed.; Elsevier, 2020, pp. 557578. DOI: .
(16) Burns, P. C.; Miller, M. L.; Ewing, R. C. U^{6+} minerals and inorganic phases; a comparison and hierarchy of crystal structures. *Can. Mineral.* **1996**, *34*, 845−880.
(17) Baker, R. J. Uranium minerals and their relevance to long term storage of nuclear fuels. *Coord. Chem. Rev.* **2014**, *266*−*267* (1), 123−136.
(18) Burns, P. C. U^{6+} minerals and inorganic compounds: Insights into an expanded structural hierarchy of crystal structures. *Can. Mineral.* **2005**, *43* (6), 1839−1894.
(19) Zhang, Y.; Lu, K. T.; Zheng, R. Synthetic uranium oxide hydrate materials: Current advances and future perspectives. *Dalton Trans.* **2022**, *51* (6), 2158−2169.
(20) Vochten, R.; Van Haverbeke, L.; Sobry, R. Transformation of schoepite into uranyl oxide hydrates of the bivalent cations Mg^{2+}, Mn^{2+} and Ni^{2+}. *J. Mater. Chem.* **1991**, *1* (4), 637−642.
(21) Burns, P. C.; Hill, F. C. A new uranyl sheet in $K_5[(UO_2)_{10}O_8(OH)_9](H_2O)$: New insight into sheet anion-topologies. *Can. Mineral.* **2000**, *38* (1), 163−173.
(22) Olds, T. A.; Plášil, J.; Kampf, A. R.; Spano, T.; Haynes, P.; Carlson, S. M.; Burns, P. C.; Simonetti, A.; Mills, O. P. Leesite, $K(H_2O)_2[(UO_2)_4O_2(OH)_5]\cdot 3H_2O$, a new K-bearing schoepite-family mineral from the Jomac mine, San Juan County, Utah, U.S.A. *Am. Mineral.* **2018**, *103* (1), 143−150.
(23) Rogova, V. P.; Belova, L. N.; Kiziyarov, G. N.; Kuznetsova, N. N. Bauranoite and metacalciouranoite, new minerals of the hydrous uranium oxides group. *Int. Geol. Rev.* **1974**, *16* (2), 214−219.
(24) Pagoaga, M. K.; Appleman, D. E.; Stewart, J. M. Crystal structures and crystal chemistry of the uranyl oxide hydrates becquerelite, billietite, and protasite. *Am. Mineral.* **1987**, *72*, 1230−1238.
(25) Li, Y.; Burns, P. C. Investigations of crystal-chemical variability in lead uranyl oxide hydrates. II. Fourmarierite. *Can. Mineral.* **2000**, *38* (3), 737−749.
(26) Olds, T. A.; Plášil, J.; Kampf, A. R.; Škoda, R.; Burns, P. C.; Čejka, J.; Bourgoin, V.; Boulliard, J.-C. Gauthierite, KPb-$[(UO_2)_7O_5(OH)_7]\cdot 8H_2O$, a new uranyl-oxide hydroxy-hydrate mineral from Shinkolobwe with a novel uranyl-anion sheet-topology. *Eur. J. Mineral.* **2017**, *29* (1), 129−141.
(27) Lu, K. T.; Zhang, Y.; Wei, T.; Ablott, T. A.; Nguyen, T. H.; Zheng, R. Synthesis and characterization of a uranium oxide hydrate framework with Sr(II) ions: Structural insights and mixed uranium valences. *New J. Chem.* **2022**, *46*, 1371−1371.
(28) Zhang, Y.; Čejka, J.; Lumpkin, G. R.; Trong Tran, T.; Aharonovich, I.; Karatchevtseva, I.; Price, J. R.; Scales, N.; Lu, K. Hydrothermal synthesis, structures and properties of two uranyl oxide hydroxyl hydrate phases with Co(II) or Ni(II) ions. *New J. Chem.* **2016**, *40*, 5357−5357.
(29) Li, Y.; Burns, P. C. Synthesis and crystal structure of a new Pb uranyl oxide hydrate with a framework structure that contains channels. *Can. Mineral.* **2000**, *38* (6), 1433−1441.
(30) Zhang, Y.; Aughterson, R.; Karatchevtseva, I.; Kong, L.; Tran, T. T.; Čejka, J.; Aharonovich, I.; Lumpkin, G. R. Uranyl oxide hydrate phases with heavy lanthanide ions: $[Ln(UO_2)_2O_3(OH)]\cdot 0.5H_2O$ (Ln = Tb, Dy, Ho and Yb). *New J. Chem.* **2018**, *42* (15), 12386−12393.
(31) Kubatko, K.-A.; Burns, P. C. Cation−Cation Interactions in $Sr_5(UO_2)_{20}(UO_6)_2O_{16}(OH)_6(H2O)_6$ and $Cs(UO_2)_9U_3O_{16}(OH)_5$. *Inorg. Chem.* **2006**, *45* (25), 10277−10281.
(32) Ablott, T. A.; Lu, K. T.; Wei, T.; Zhang, Y. Exploring the influence of pH on the structural intricacies of uranium oxide hydrates containing both Cd(II) and K(I) ions. *Dalton Trans.* **2023**, *52* (20), 6629−6640.
(33) Ablott, T. A.; Lu, K. T.; Aughterson, R. D.; Zhang, Y. Uranium oxide hydrate frameworks with Er(III) or Y(III) ions: Revealing structural insights leading to the low symmetry. *Dalton Trans.* **2022**, *51* (41), 15965−15973.
(34) Lu, K. T.; Zhang, Y.; Wei, T.; Wang, Z.; Oldfield, D. T.; Zheng, R. Hydrothermal Syntheses of Uranium Oxide Hydrate Materials with Sm(III) Ions: pH-Driven Diversities in Structures and Morphologies and Sm-Doped Porous Uranium Oxides Derived from Their Thermal Decompositions. *Inorg. Chem.* **2021**, *60* (17), 13233−13241.
(35) Lu, K. T.; Zhang, Y.; Aughterson, R. D.; Zheng, R. Uranyl oxide hydrate frameworks with lanthanide ions. *Dalton Trans.* **2020**, *49* (44), 15854−15863.
(36) Krivovichev, S. V.; Plášil, J. Mineralogy and crystallography of uranium, In *Uranium: Cradle to Grave*, Burns, P. C.; Sigmon, G. E. ed.; Mineralogical Association of Canada, 2013, Vol. *43*, pp. 15119. DOI: .
(37) *mineralogy of Zinc*. https://www.mindat.org/. (accessed 15 January 2024).
(38) Zhang, Y.; Lu, K. T.; Wei, T.; Karatchevtseva, I.; Zheng, R. Filling the gaps of uranium oxide hydrates with magnesium(II) ions: Unique layered structures and the role of additional sodium(I) ions. *Dalton Trans.* **2023**, *52* (47), 17942−17953.
(39) Hill, F. C.; Burns, P. C. The structure of a synthetic Cs uranyl oxide hydrate and its relationship to compreignacite. *Can. Mineral.* **1999**, *37* (5), 1283−1288.
(40) Rivenet, M.; Vigier, N.; Roussel, P.; Abraham, F. $[Ni(H_2O)_4]_3[U(OH,H_2O)(UO_2)_8O_{12}(OH)_3]$, crystal structure and comparison with uranium minerals with U_3O_8-type sheets. *J. Solid State Chem.* **2009**, *182* (4), 905−912.
(41) Chernorukov, N. G.; Nipruk, O. V.; Klinshova, K. A.; Tumaeva, O. N.; Sokolov, D. V. A family of uranyl oxide hydrate phases with bivalent cations $[M^{II}(H_2O)_4][(UO_2)_3O_3(OH)_2]\cdot H_2O$ (M^{II} − Mn, Co, Ni, Zn): Synthesis, characterization and chemical stability in aqueous solutions. *New J. Chem.* **2021**, *45*, 9922−9935.
(42) Aragão, D.; Aishima, J.; Cherukuvada, H.; Clarken, R.; Clift, M.; Cowieson, N. P.; Ericsson, D. J.; Gee, C. L.; Macedo, S.; Mudie, N.; et al. MX2: A high-flux undulator microfocus beamline serving both the chemical and macromolecular crystallography communities at the Australian Synchrotron. *J. Synchrotron Radiat.* **2018**, *25* (3), 885−891.
(43) Kabsch, W. Integration, scaling, space-group assignment and post-refinement. *Acta Crystallogr., Sect. D: Biol. Crystallogr.* **2010**, *66* (2), 133−144.
(44) Sheldrick, G. M. *SADABS, Empirical Absorption and Correction Software*; University of Göttingen: Göttingen, 1996.
(45) Sheldrick, G. M. SHELXT − Integrated space-group and crystal-structure determination. *Acta Crystallogr., Sect. A: Found. Adv.* **2015**, *71* (1), 3−8.
(46) Sheldrick, G. M. Crystal structure refinement with SHELXL. *Acta Crystallogr., Sect. C: Struct. Chem.* **2015**, *71* (1), 3−8.
(47) Dolomanov, O. V.; Bourhis, L. J.; Gildea, R. J.; Howard, J. A. K.; Puschmann, H. OLEX2: A complete structure solution, refinement and analysis program. *J. Appl. Crystallogr.* **2009**, *42* (2), 339−341.
(48) Coelho Software. *TOPAS-Academic V5*; Coelho Software: Brisbane, 2012.
(49) Lu, K. T.; Zhang, Y.; Wei, T.; Čejka, J.; Zheng, R. Layer-structured uranyl-oxide hydroxy-hydrates with Pr(III) and Tb(III) ions: Hydroxyl to oxo transition driven by interlayer cations. *Dalton Trans.* **2020**, *49* (18), 5832−5841.
(50) Weng, Z.; Wang, S.; Ling, J.; Morrison, J. M.; Burns, P. C. $(UO_2)_2[UO_4(trz)_2](OH)_2$: A U(VI) Coordination Intermediate

https://doi.org/10.1021/acsomega.4c06188
ACS Omega 2024, 9, 38284−38294

between a Tetraoxido Core and a Uranyl Ion with Cation−Cation Interactions. *Inorg. Chem.* **2012**, *51* (13), 7185−7191.
(51) Shannon, R. D. Revised effective ionic radii and systematic studies of interatomic distances in halides and chalcogenides. *Acta Crystallogr., Sect. A: Found. Adv.* **1976**, *32* (5), 751−767.
(52) Plasil, J. The crystal structure of uranyl-oxide mineral schoepite, $[(UO_2)_4O(OH)_6](H2O)_6$, revisited. *J. Geosci.* **2018**, *63* (1), 65−73.
(53) Zhang, Y.; Wei, T.; Tran, T. T.; Lu, K.; Zhang, Z.; R. Price, J.; Aharonovich, I.; Zheng, R. $[U(H_2O)_2]\{[(UO_2)_{10}O_{10}(OH)_2][(UO_4)(H_2O)_2]\}$: A Mixed-Valence Uranium Oxide Hydrate Framework. *Inorg. Chem.* **2020**, *59* (17), 12166−12175.
(54) Frost, R. L.; Čejka, J.; Ayoko, G. A.; Weier, M. L. Vibrational spectroscopic study of hydrated uranyl oxide: Curite. *Polyhedron* **2007**, *26* (14), 3724−3730.
(55) Frost, R. L.; Čejka, J.; Weier, M. L. Raman spectroscopic study of the uranyl oxyhydroxide hydrates: becquerelite, billietite, curite, schoepite and vandendriesscheite. *J. Raman Spectrosc.* **2007**, *38* (4), 460−466.
(56) Zhang, Y.; Ablott, T. A.; Nicholas, M. K.; Karatchevtseva, I.; Plášil, J. Capturing ammonium nitrate in a synthetic uranium oxide hydrate phase: Revealing the role of ammonium ions and anion inclusions. *Dalton Trans.* **2024**, *53* (26), 11112−11119.

https://doi.org/10.1021/acsomega.4c06188
ACS Omega 2024, 9, 38284−38294